Room Temperature Lead-free Multiaxial Inorganic-organic Hybrid Ferroelectric

Bin Wang#, Dangwu Ma#, Haixia Zhao, Lasheng Long* and Lansun Zheng*

Collaborative Innovation Center of Chemistry for Energy Materials, State Key Laboratory of Physical Chemistry of Solid Surfaces and Department of Chemistry, College of Chemistry and Chemical Engineering, Xiamen University, Xiamen 361005, P. R. China.

*Correspondence and requests for materials should be addressed to H.-X. Zhao and L.-S. Long (E-mail: hxhzao@xmu.edu.cn, lslong@xmu.edu.cn).

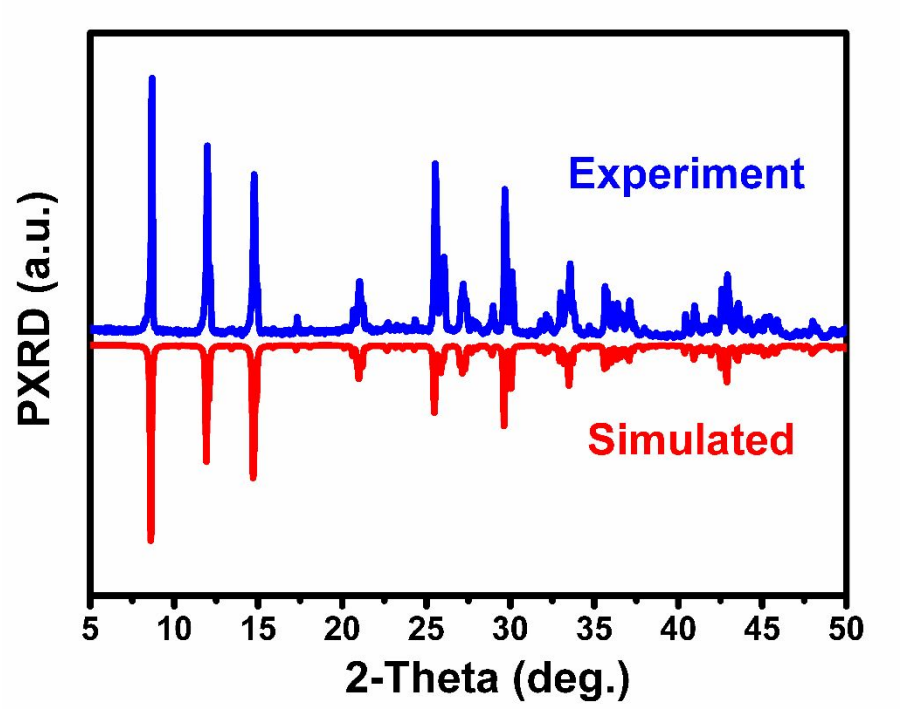

Figure S1. PXRD patterns of **1** at 300 K.

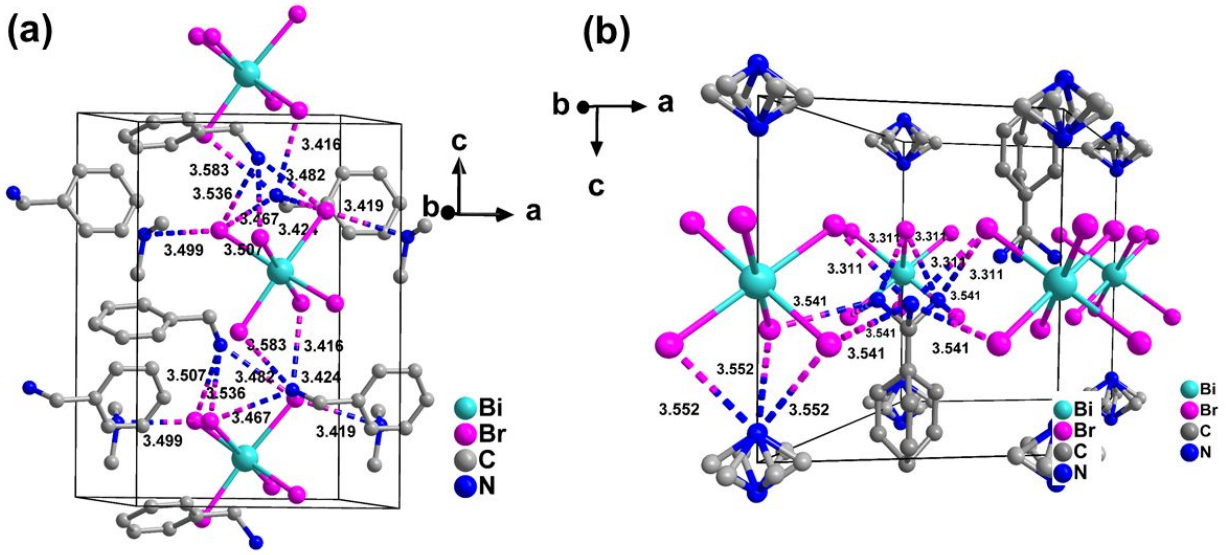

Figure S2. The distance (Å) between the acceptors (Br) and donors (N) in LTP (a) and HTP (b) of **1**.

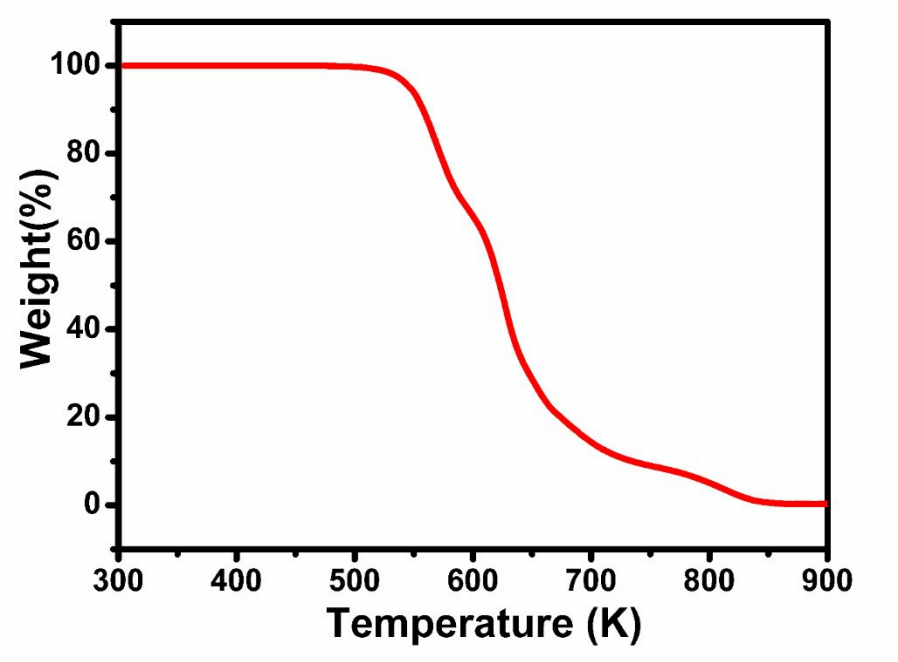

Figure S3. TG curve of **1** with heating rate of 10 K·min^{-1}, indicating a high thermal stability up to 500 K.

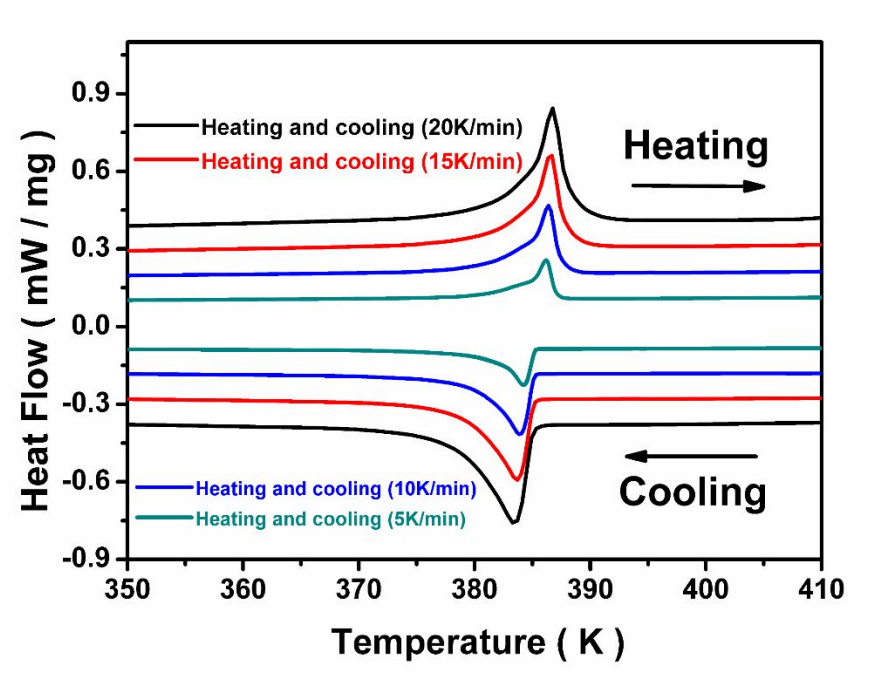

Figure S4. DSC curves of **1** at different scanning rates.

Differential scanning calorimetry (DSC) measurements were performed on a PerkinElmer Diamond DSC with heating and cooling rates of 5, 10, 15 and 20 $K \cdot min^{-1}$ (the mass of the sample is 11.40 mg) under nitrogen atmospheres.

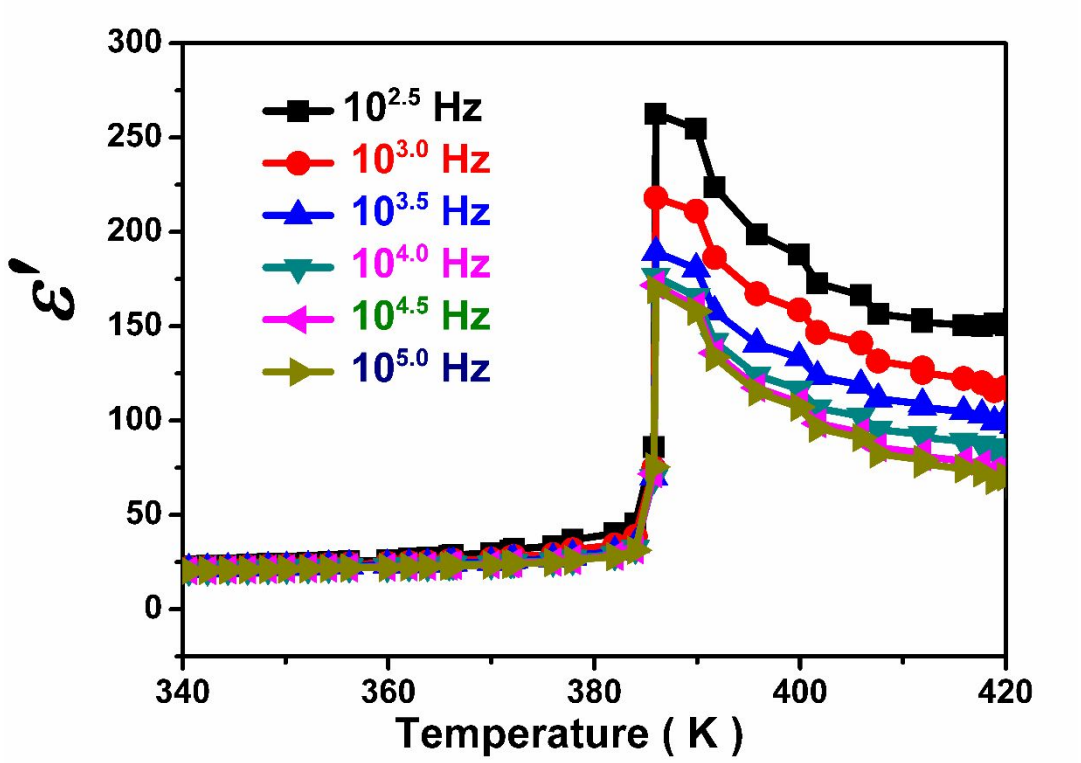

Figure S5. The temperature dependence of dielectric real parts (ε′) for **1** at different frequencies.

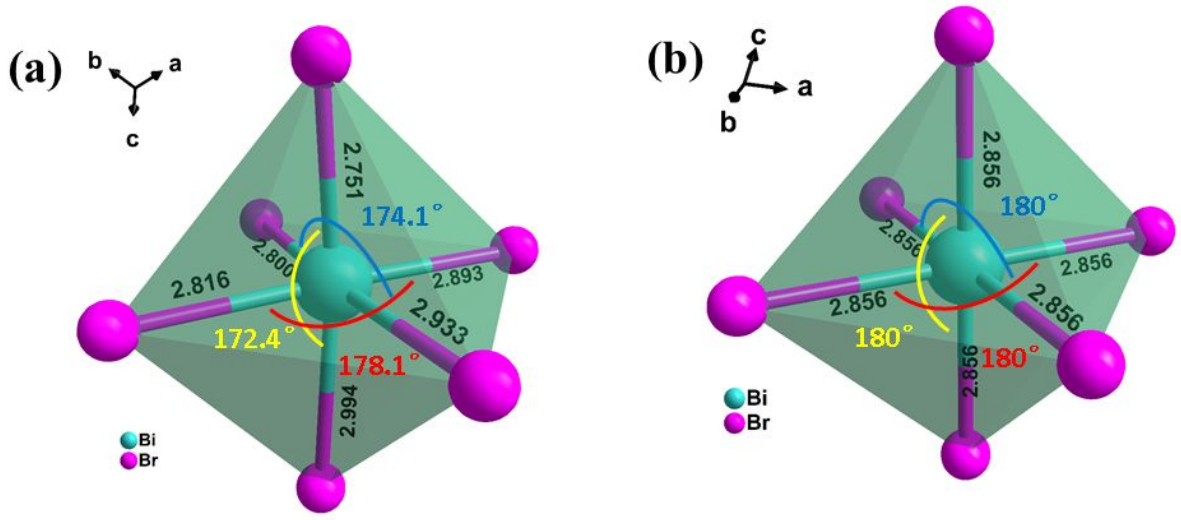

Figure S6. The comparison of $BiBr_6$ octahedron in LTP (a) and HTP (b) of **1**.

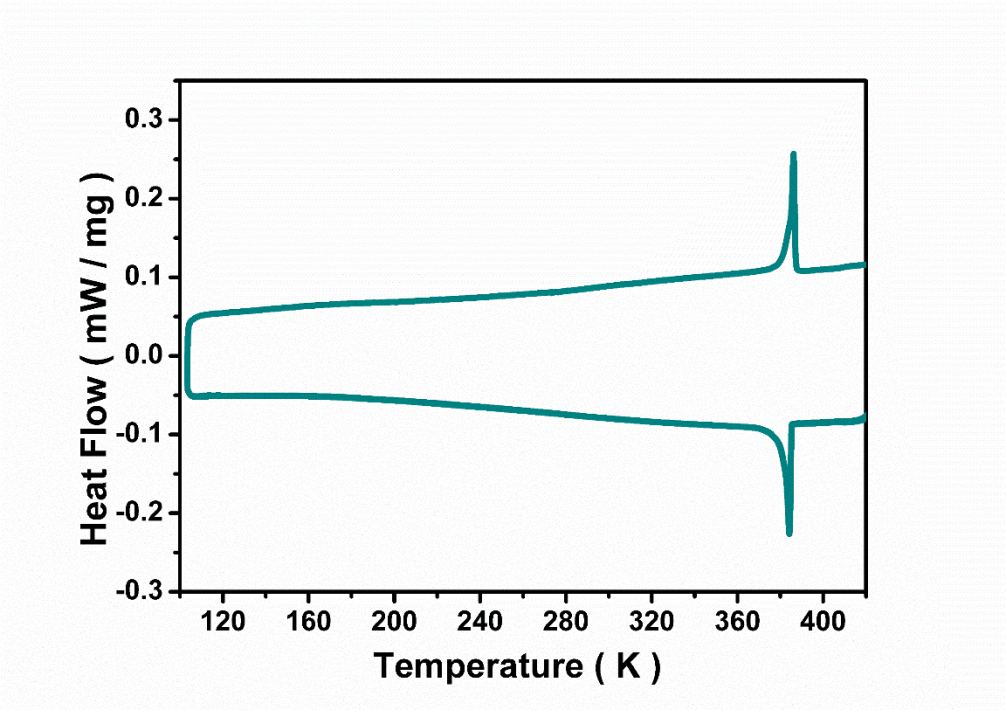

Figure S7. DSC curves of **1** at temperature range 100 K to 425 K.

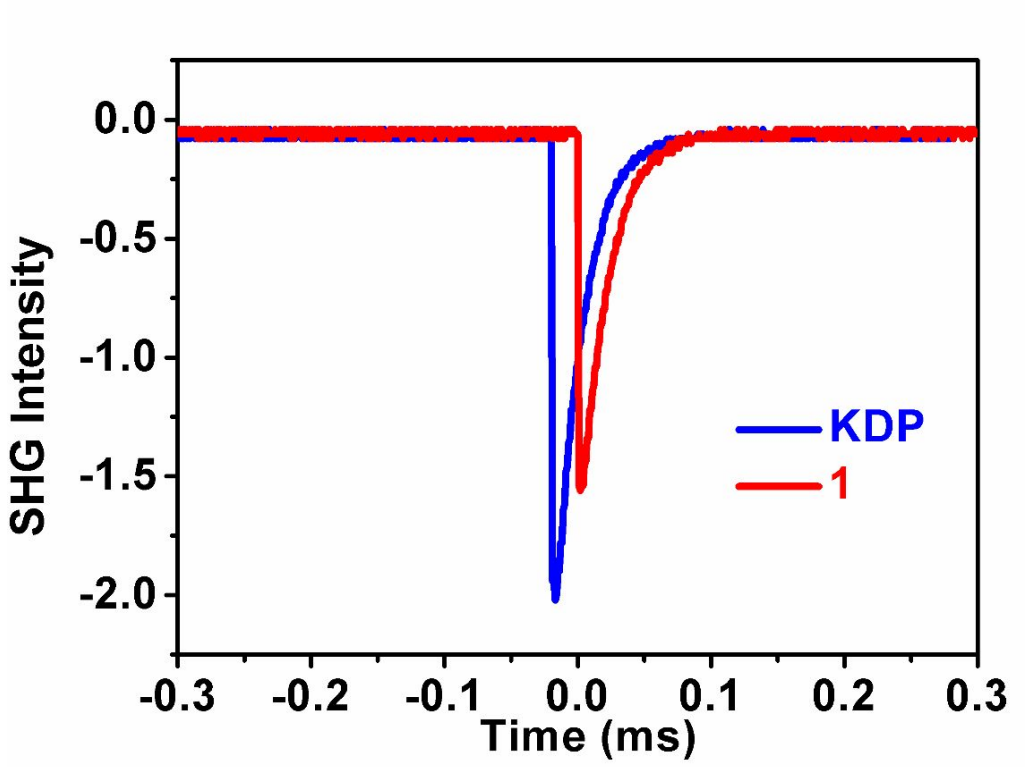

Figure S8. Oscilloscope traces of SHG signals for **1** and KDP

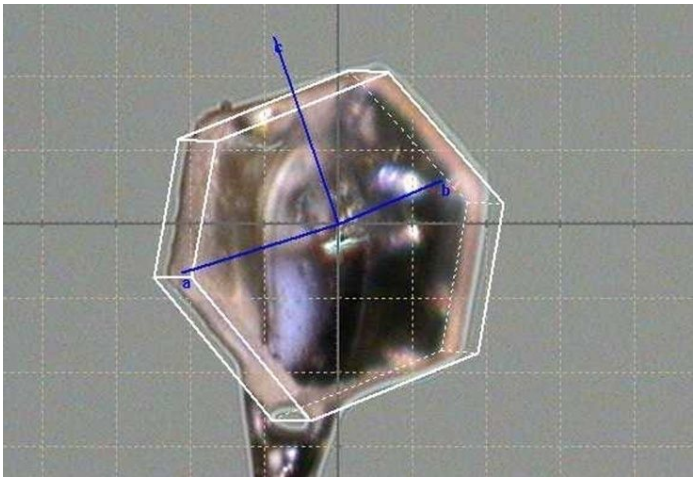

Figure S9. The plate surface of the signal crystal **1** and the orientation of the crystal is determined by a data analysis software of Agilent Supernova CCD diffractometer.

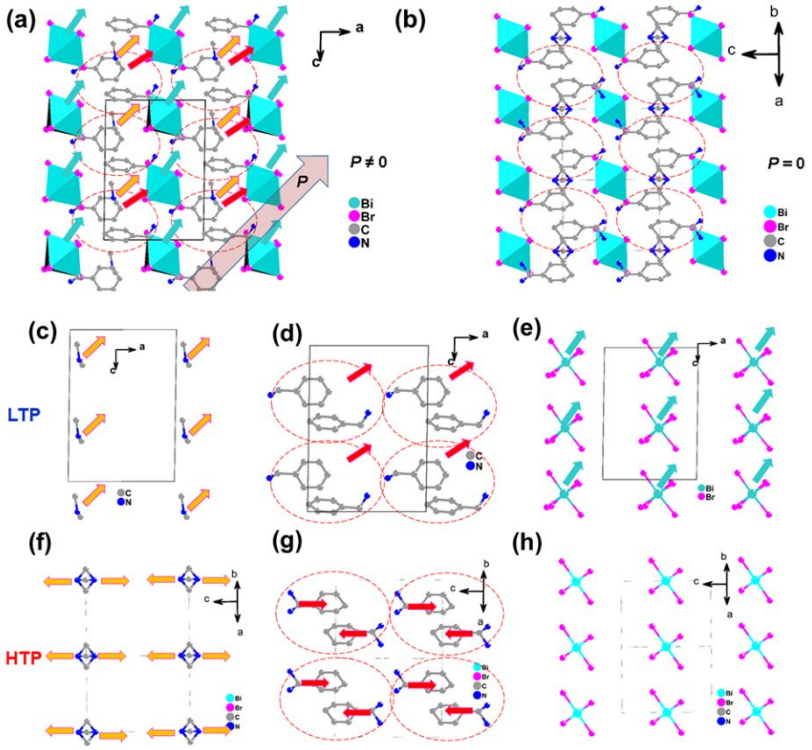

Figure S10. Crystal packing of **1** viewed along the *b*-axis direction in the (a) LTP and the same view in the (b) HTP. The projection of LTP (c, d, e) and HTP (f, g, h) on *ac* plane are divided into three parts for the convenience of analysis and discussion.

In order to show the overall polarity, the projection of LTP and HTP on *ac* plane are divided into three parts for the convenience of analysis and discussion. As depicted in Figure S10c and S10d, all the C-N bonds of the $C_6H_5CH_2NH_3^+$ and $(CH_3)_2NH_2^+$ cations align along a certain direction on the *ac* plane. Meanwhile, inorganic $BiBr_6$ octahedra with a sterically distorted configuration also leads to the displacements of negatively charged centers along a certain direction on the *ac* plane (Figure S10e). Consequently, the combination of dynamic movement of organic and inorganic cations gives rise to dipoles along a certain direction on the *ac* plane, thereby resulting in nonzero net spontaneous polarization, which suggests the possible ferroelectricity of **1** (Figure S10a). In the HTP, **1** crystallizes in centrosymmetric space group *P*-3*m*1. For organic cations, the $C_6H_5CH_2NH_3^+$ and $(CH_3)_2NH_2^+$ cations become highly disordered in the HTP (Figure S10f and S10g). And the inorganic $BiBr_6$ octahedra exhibits a sterically regular configuration (Figure S10h). These results satisfy the demands of crystallographic symmetry, leading to a zero net

spontaneous polarization (Figure S10b). Therefore, thermally triggered order−disorder dynamic transformation of organic cations and displacement of inorganic Bi atoms synergistically lead to ferroelectric-paraelectric phase transition behavior of **1**. The overall polarity of the structure line up in the crystallographic structure as shown in Figure S10a.

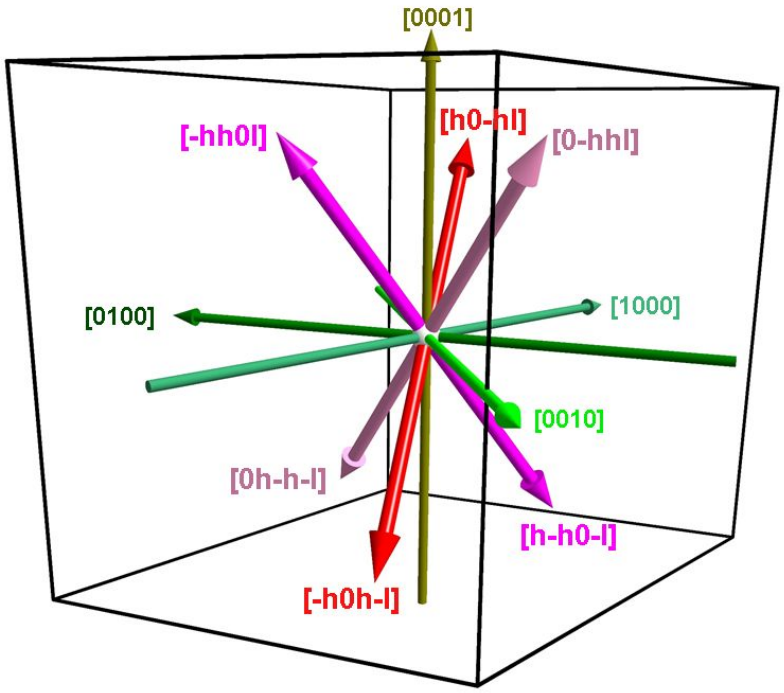

Figure S11. The scheme drawing of possible equivalent polarization directions in the LTP of **1**.

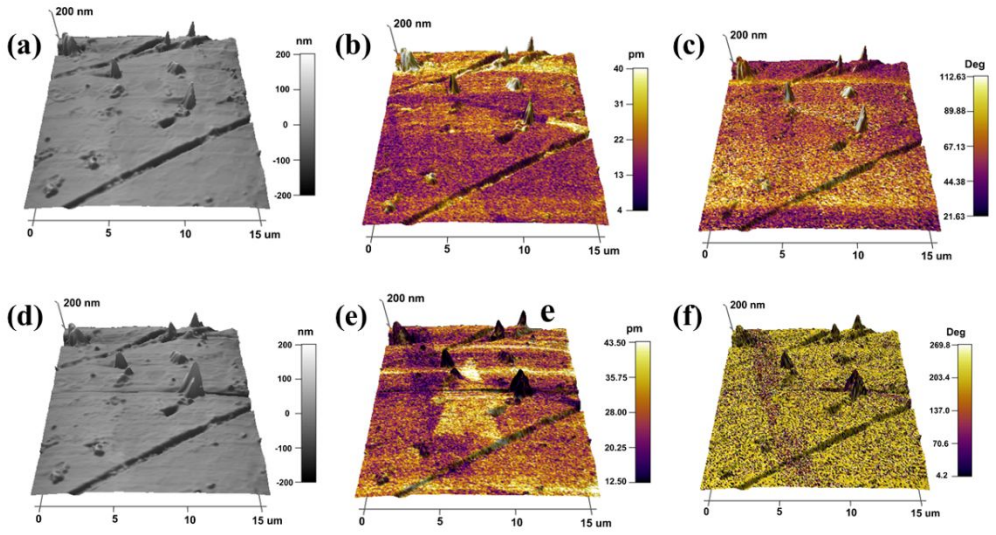

Figure S12. Polarization reversal was measured by a single crystal sample of **1**. Topographic images (a), vertical PFM amplitude image (b) and vertical PFM phase images (c) of the crystal surface overlaid on 3D topography in initial state. Topography image (d), vertical PFM amplitude image (e) and vertical PFM phase image (f) overlaid on 3D topography recorded after writing a star area with +80/-80 V.

Table S1. Crystal data of **1** at 300 K.

Compound	$[(CH_3)_2NH_2]$ $[C_6H_5CH_2NH_2]_2BiBr_6$ (1)
temperature (K)	300.01(10)
phase	LTP
formula weight	950.85
crystal system	monoclinic
space group	*Pc*
a (Å)	10.2649(2)
b (Å)	8.6093(2)

c (Å)	14.6506(3)
α (deg)	90
β (deg)	90.408(2)
γ (deg)	90
volume (Å^3)	1294.70(5)
Z	2
scan mode	ω-scan
μ (mm^{-1})	24.264
F(000)	876.0
crystal size (mm^3)	0.18 × 0.15 × 0.06
radiation	Mo Kα
wavelength (Å)	0.71073
2θ range for data collection (deg)	8.614-137.322
index ranges	−11 ≤ h ≤ 12, −9 ≤ k ≤ 10, −17 ≤ l ≤ 17
density (g cm^{-3})	2.439
reflections collected	7892
R_{int}	0.0410
refinement method	full-matrix least-squares on F^2
data/restraints/parameters	3839/11/215
goodness-of-fit on F^2	1.050
R_1, ωR_2 [$I > 2\sigma(I)$]	0.0656, 0.1684
R_1, ωR_2 [all data]	0.0664, 0.1691
ρ_{max}, ρ_{min} (e Å^{-3})	1.15, -2.35

[a] $R_1 = \sum||F_o| - |F_c||/\sum|F_o|$, $\omega R_2 = \{\sum[\omega(|F_o|^2 - |F_c|^2)]/\sum[\omega|F_o|^4]\}^{1/2}$ and $\omega = 1/[\sigma^2(F_o^2) +$

$(0.0885P)^2+28.1926P]$.